Static and dynamic behavior of 360° domain walls in patterned thin films

A. L. Gonzalez Oyarce,[1,*] Y. Nakatani,[2] and C. H. W. Barnes[1]
[1]*Cavendish Laboratory, Thin Film Magnetism Group, Cambridge, CB3 0HE, United Kingdom*
[2]*University of Electro-communications, Chofu 182-8585, Japan*
(Received 2 March 2013; published 4 June 2013)

We study the static and dynamic behavior of transverse domain walls and 360° domain walls in a thin film of isotropic material including pinning effects caused by geometric defects in the form of triangular antinotches. In terms of the static interaction, our model reduces the domain walls to sources of magnetic charge, allowing an electrostatic-like description of their interaction. Such a concept was applied to both of these magnetic textures allowing us to estimate the shortest distance between the antinotches at which the domains walls can be located, while still being pinned. Regarding the domain walls' dynamical behavior, accurate micromagnetic simulations of our system were performed, characterizing their recombination times as well as showing that triangular notches allow the coherent movement of single and arrays of 360° domain walls by pulses of spin current. This behavior could not be observed in single transverse walls given the long-range interaction that they present, impeding coherent domain wall motion. These findings allow us to estimate the maximum 360° domain wall density, observing an increase by a factor of four when compared to systems based on single transverse domain walls, which potentially gives our system important industrial applications.

DOI: 10.1103/PhysRevB.87.214403 PACS number(s): 75.60.Ch, 75.78.Fg, 75.78.Cd

I. INTRODUCTION

The use of transverse domain walls (TDWs) in magnetic nanostructures has found some important applications in data storage devices.[1–7] The memory device proposed by Konishi[1] uses two vertical block lines to represent 1 bit, which is based on an oval racetrack where the domain walls were written and read in different segments of the track, whereas the racetrack memory proposed by Parkin *et al.*[8] is based on plane TDWs that are driven along open tracks. The limitation of TDWs is the long-range stray field that they produce, making them susceptible to interactions with other magnetic and geometric structures over a range of several microns.[2,9–13] In an effort to overcome this problem, a composite object made of two TDWs, the 360° domain wall (360° DW) has been proposed as an alternative, by Gonzalez *et al.*[14] and Muratov *et al.*[15] The general behavior of 360° DWs is described in Refs. 14 and 16–18, their weaker stray field as compared to TDWs being one of their main characteristics,[9,19] as the 360° DWs are composed of two TDWs, forming an almost closed magnetic flux structure.[20,21]

In this paper we use a Permalloy (Py) patterned surface with triangular notches placed every 235, 352, or 470 nm, center-to-center distance, with 360° DWs already nucleated at the notches as shown in Fig. 1. The distance between the notches is approximately one, one and a half, and two times the 360° DW length. Using the interaction model developed by Allwood *et al.*,[12,22] which considers TDWs as magnetic textures composed only of magnetic charges centered at their middle point, we were able to describe the static behavior of TDWs and 360° DWs in this system. Allwood *et al.*[6] experimentally established that transverse domain walls could be modeled as point sources of magnetic charge, and that the interaction between two TDWs is analogous to electric charges interacting. Based on this concept, we compared the interaction between two TDWs with the interaction between a pair of 360° DWs, finding that it mainly originates from the stray field produced by these magnetic textures. It is important to note that for shorter distances, which is close to two domain wall lengths in the case of 360° DWs, the model loses validity. At these distances the interaction between the domain walls modifies their structure, and short-range interactions such as the exchange energy become relevant. From this analysis we can estimate the minimum distance at which two 360° DWs can be nucleated while still being pinned by the triangular notches. In terms of the dynamic behavior of TDWs and 360° DWs we characterized the movement of a single 360° DW under a spin current in the patterned Py stripe, and then we expanded the description to an array of four TDWs or four 360° DWs, finding that only 360° DWs are suitable for manipulation under these conditions. Moreover, we characterized their typical recombination times, finding the DW-to-DW distances at which the 360° DWs could be unpinned from the antinotches and moved from one position to another in a coherent fashion.

This proposed system could be the basis for a device where binary bits could be determined by the presence or absence of 360° DWs. In this report we achieve a DW density ∼4 times higher compared to the devices reported by Parkin,[3] where only 1 TDW per micron can be stored and manipulated. At domain wall densities higher than 1 TDWs per micron, the TDWs interact, combining or annihilating depending on their chirality.[20] Furthermore, in a device with these characteristics there could be two possible ways of injecting 360° DWs into the patterned structure. The first one could be to nucleate them locally on top of the antinotches,[23] having the advantage of creating any arrangement of 360° DWs which could be moved across the patterned structure. Alternatively 360° DW injection could be accomplished by nucleating them at the ends of the stripe with a specially designed pad and then transferring them to the notches. This technique has already been demonstrated by Ross *et al.*[24] and Diegel *et al.*[25] using a circular structure attached to a Py nanostripe, where they were able to inject 360° DWs (and/or any multiplier of a TDWs) into the nanostripe. Regarding the pinning properties of this system, we found

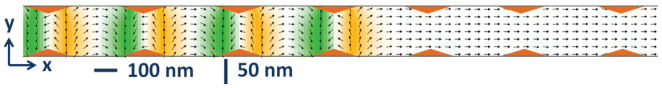

FIG. 1. (Color online) Graphical representation of the initial conditions, where four 360° DWs were placed in the notches, which later were moved using a spin current.

that for the deeper notches a higher spin current was needed to unpin the walls, but this also implied that a shorter spin current pulse had to be used in order to accurately move the 360° DWs from one stable position to the next. Moreover, our proposed system uses a current of ∼5 pA/m, which is close to what could be obtained under standard experimental conditions.

The remainder of this paper is organized as follows. In Sec. II we describe the parameters and numerical methods used in this study. Furthermore, in Sec. III, we present the results of the static regime, notch characterization, and the dynamical regime. Finally, in Sec. IV, we summarize the highlights of our findings and give an outlook of this research.

II. METHODOLOGY AND SIMULATION DETAILS

In this paper we simulated a Py stripe with a thickness 4 nm, width 100 nm, with periodic boundary conditions in the x direction, with no magnetocrystalline anisotropy, and patterned with 7 triangular notches. The cell size used for the simulations was of 4.0 nm in the x direction and 2.5 nm in the y direction. The initial state assumed a number of 360° DWs nucleated at the notches, as shown in Fig. 1. The simulations were carried out using the simulations package OOMMF and its extension for spin current[26–29] which is based on the micromagnetic energy functional $E(\mathbf{M})$, Eq. (1),

$$E(\mathbf{M}) = \int_{\Omega} \left(\frac{A}{M_s^2} |\nabla \mathbf{M}|^2 - \mu_0 \mathbf{H}_Z \cdot \mathbf{M} \right) d^3\mathbf{r} + \mu_0 \int_{\mathrm{R}^3} \mathbf{H}_d(\mathbf{r}) \cdot \mathbf{M}(\mathbf{r}) d^3\mathbf{r}, \quad (1)$$

with H_d, the demagnetizing field, given by $H_d = -\nabla\Phi$,

$$\Phi = -\frac{1}{4\pi} \int_V \frac{\rho(\mathbf{r}')}{|\mathbf{r} - \mathbf{r}'|} d^3\mathbf{r}' + \frac{1}{4\pi} \int_{\Omega} \frac{\sigma(\mathbf{r}')}{|\mathbf{r} - \mathbf{r}'|} d\mathbf{r}'. \quad (2)$$

In Eq. (1) the first term is the exchange energy, the second, the Zeeman energy, and the third term corresponds to the demagnetizing energy. Furthermore, in Eq. (2), $\rho(\mathbf{r}) = -\nabla \cdot \mathbf{M}_s(\mathbf{r})$ and $\sigma(\mathbf{r}) = \mathbf{M}_s(\mathbf{r}) \cdot \mathbf{n}$ are the volume and surface magnetic charges, respectively.[30] The values of the constants used are the standard for Py, where A is the exchange constant with a value of 13 pJ/m, $M_s = 860$ kA/m; moreover, we considered $K = \mu_o M_s^2/2$. Hence L_{ex}, the exchange length, is defined by $L_{ex} = \sqrt{A/K} = 5.289$ nm.[31]

As we are interested in studying the dynamical behavior of the 360° DWs in such patterned structures, we applied a spin-polarized current in the shape of a time step function in order to induce the translational motion of the walls, as homogeneous magnetic fields are not capable of moving this kind of magnetic texture.[32] The time evolution of the system is based on the description given by Eq. (3), which is the Landau-Lifshitz-Gilbert including the spin current non-adiabatical term,[33] where H is obtained from $H = -\nabla E(\mathbf{M})$. The parameters α and β are the damping parameter and the non-adiabatical spin transfer torque, respectively, being set to $\alpha = 0.01$ and $\beta = 2\alpha = 0.02$; see Eq. (3). Furthermore, in order to describe the effect of the spin current on the pinned 360° DWs, we varied the amplitude, the duration of the pulse, and the relaxation time after the pulse was applied:

$$\dot{\mathbf{m}} = \gamma_0 \mathbf{H} \times \mathbf{m} + \alpha \mathbf{m} \times \dot{\mathbf{m}} - (\mathbf{u} \cdot \nabla)\mathbf{m} + \beta \mathbf{m} \times [(\mathbf{u} \cdot \nabla)\mathbf{m}]. \quad (3)$$

III. RESULTS

In this notched patterned system we address the static and dynamic interaction between TDWs as well as between 360° DWs. Having a complete description will not only allow us to have a better understanding of the inherent properties of these magnetic domain walls, but it will also allow the calculation of the minimum distances at which the DWs can be located while still being pinned by the triangular notches. In order to accomplish such goals, we identified two regimes. The first regime corresponds to the static case where DWs are located at the notches and their interaction with each other comes mainly from their demagnetizing field. The second regime is the dynamical case where the DWs have translational movement in addition to their interaction through the demagnetizing field. In order to have a better comprehension of the behavior of DWs in this system, the pinning effects of the notches were characterized. We address the static regime first in Sec. III A, the notch characterization in Sec. III B, and then the dynamical regime of single and multiple 360° DWs in Secs. III C–III E.

A. Static regime

The static regime comprises the behavior of domain walls when they are pinned at the notches. In this section we compare the interaction energy of the 360° DWs with the TDW case. From this analysis we can estimate the minimum distance at which two 360° DWs can be nucleated, while still being pinned by the triangular notches. To carry out such comparison, we consider the simplified picture where the TDWs and 360° DWs are structures made only of surface and volume magnetic charges, named σ and π, respectively,[12,22] as shown in Fig. 2. In the case of two interacting TDWs we discarded the contribution of the π charges as they provide a dipole Coulomb-type effective potential, which decreases faster over distances when compared with the monopole Coulomb-type of the σ charges. The interaction energy between two σ charges, by E_{mon}, which resembles the interaction of two electric monopoles, is given by $E_{\mathrm{mon}} = \frac{\sigma_i \sigma_j}{4\pi\mu_0\Delta}$, where

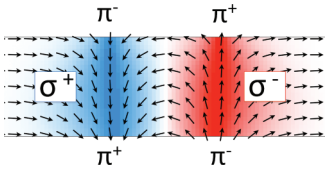

FIG. 2. (Color online) Graphical representation of the charge model superimposed to the typical distribution of the magnetization across a 360° DW. The magnetization in the $-y$ direction is shown in blue and the magnetization in the $+y$ direction is shown in red.

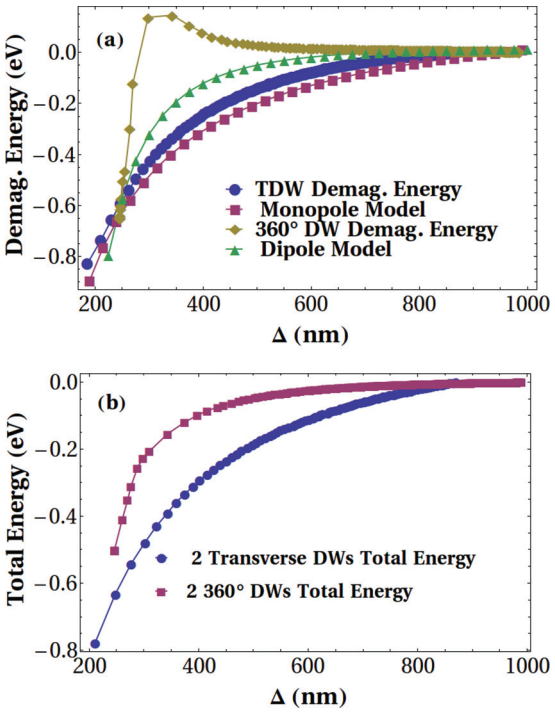

FIG. 3. (Color online) Demagnetizing energy in function of the separation between two TDWs and two 360° DWs. The zero of such energy was adjusted in order to make the comparison.

$\sigma_i = \pm 2\mu_0 M_s wt$, w being the width of the stripe, t its thickness, and Δ the distance between the TDWs.[12,22] In the case of 360° DWs, we again discarded the contribution of the π charges, as shown in Fig. 2, because they provide an effective quadrupole potential Coulomb type that decreases faster in magnitude when compared to the effective dipole interaction generated by the σ charges. The interaction energy between two 360° DWs is then modeled as $E_{\text{dip}} = -\frac{\sigma_i \sigma_j}{4\pi\mu_0 \Delta^3}$.[12,22] The results of such calculations are shown in Fig. 3.

The results shown in Fig. 3(a) show that the proposed model of two interacting TDWs is consistent with the simulations; i.e., the demagnetizing energy is decreased as walls come closer. On the other hand, while the extreme values for the demagnetizing energy of two 360° DWs are in agreement with the σ charge dipole model proposed, the results provide some evidence that the interaction of two 360° DWs at shorter distances is of a more complex nature and thus requires a more robust model, probably including the deformation of each wall induced by the interaction. The evidence presented shows that the pinning potential of the notches located at 235 nm, 1 DW length, is sufficient to overcome the interaction between TDWs and 360° DWs, holding such DWs in place. Moreover, as the walls are compressed at the notches the magnetic charge is diminished by a quarter, reducing the effective attractive force by ∼0.56, from 0.726 eV to 0.407 eV. This is lower than the depinning energy for the three types of notches used; see Table I.

B. Notch characterization

The notches used in this system had depths of 6.25 or 12.5 nm, and widths of 117 or 171 nm. It is worth noting that notches of depth 25 nm were also used, but the 360° DWs were destroyed before being unpinned. In the characterization of the notches there are two regimes to bear in mind, the first being where there is only an isolated notch and the second, where there is an array of such structures. In the case of an isolated notch, the length of the spin current pulse required to unpin the wall is higher than in the case where there is an array of notches. In the case of a single notch, the wall is considered to be unpinned when it breaks interaction with the notch and moves freely in the direction of the spin current; this occurs at distances above five hundred nanometers. On the other hand, when there is a patterned structure with several notches on it, the length of the pulse is reduced because it is only necessary to move the DWs from one notch to another, as the DWs will get trapped at the next notch. Furthermore, in the case of several walls the interaction between DWs becomes relevant to the fabrication and design of DW-based devices. In Table I the values for the depinning spin current velocities and pulse duration needed are tabulated for isolated notches. Moreover, we consider "writing" as the time it takes to move one domain wall from one notch to another, since the presence or absence of such DWs in the notches is the basis of having a 1/0 bit. On the other hand, the term "reading" applies to the time that it takes for the wall to relax at the notch, as that time would be used to read the presence of absence of the 360° DWs at the notches.

TABLE I. Summary of geometrical and energetic properties of the notches used. The values of the depinning current are for isolated notches. For notches of depth 25.00 nm the 360° DWs were destroyed before being unpinned; hence there is neither value for the depinning current nor the pulse duration.

Depth (nm)	Width (nm)	Depinning u (m/s)	Pulse duration (ns)	Energy well (eV)
6.25	117.0	250 ± 25	2.5 ± 0.25	0.68
	171.0	250 ± 25	2.5 ± 0.25	0.69
12.50	117.0	350 ± 25	3 ± 0.5	1.7
	171.0	350 ± 25	3 ± 0.5	1.8
25.00	117.0			4.3
	171.0			4.5

C. Single 360° DW dynamics

We first considered the case of a single 360° DW, which we were able to accurately move through our system using nanosecond pulses of current. The pulse length and the spin current velocity were dependent on the depth and separation between the notches used. For example while notches of depth 6.25 nm and separation 235 nm required a pulse of length 2.5 ns and $u = 300$ m/s, a notch of depth 12.5 nm and separation 352 nm required a pulse of $u = 400$ m/s and a pulse duration of 1.25 ns. Furthermore, we found that the time for the wall to relax at the notch was approximately 3–4 ns. A typical example of this behavior is shown in Fig. 4. It is worth noting as well that DW annihilation in the steady-state regime occurs at $u = 560$ m/s, for $\alpha = 0.01$ and $\beta = 0.02$. This behavior is similar to what was reported in Ref. 32. Moreover, we observed that for values close to the critical spin current velocity of up to 700 m/s, the typical length up to which the DW annihilates is

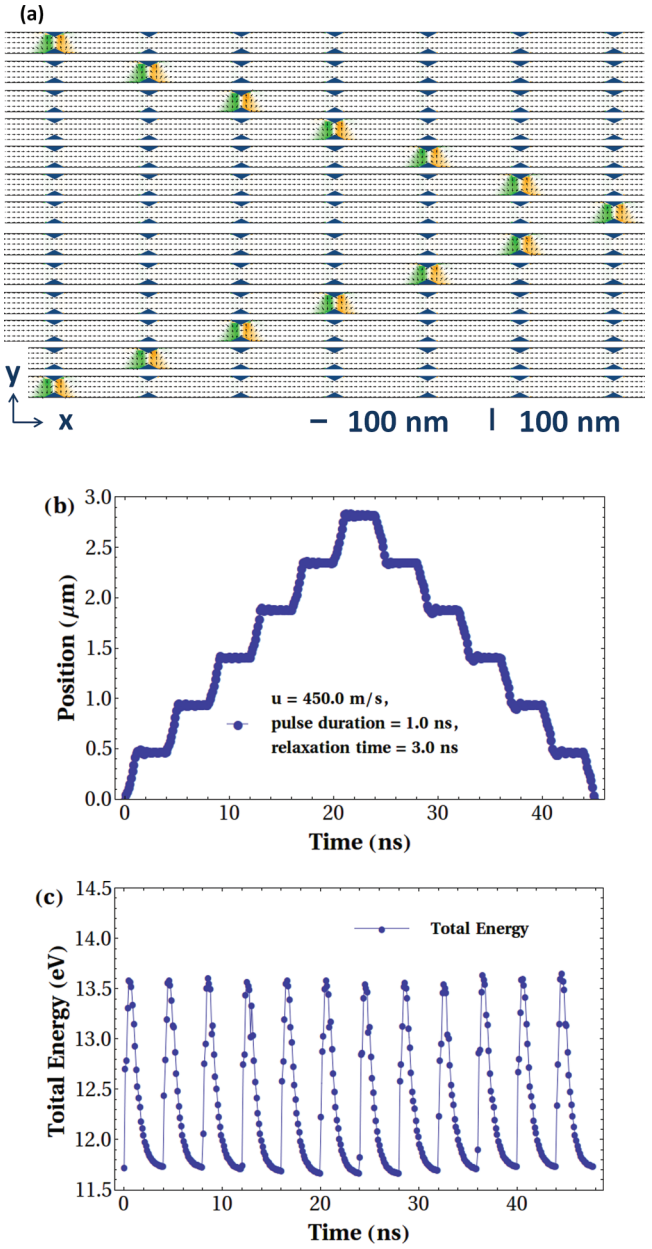

FIG. 4. (Color online) (a) Single DW movement, notch separation 470 nm, depth 12.5 nm, width 117 nm, $u = 450.0$ ms, pulse length 1.0 ns, and relaxation 3.0 ns. The magnetization pointing $-y$ is shown in green and the magnetization pointing $+y$ is shown in orange. (b) 360° DW position in time. The jumps in the position demarcate the DW movement when the spin current pulse is applied, until the next stable position is achieved. (c) Total energy of a single 360° DW during the process shown in Fig. 4(a). This shows how the notches act like potential wells for the pinning of the DWs.

about 3–4 μm. This typical annihilation length is 7 to 17 times the notch separation used in this report. This feature opens the possibility for the use of higher spin current velocities than the critical spin current in the steady state.

D. Multiple DW dynamics

For an array of four DWs, we were able to move them coherently using a spin current pulse, as shown in Fig. 5. We

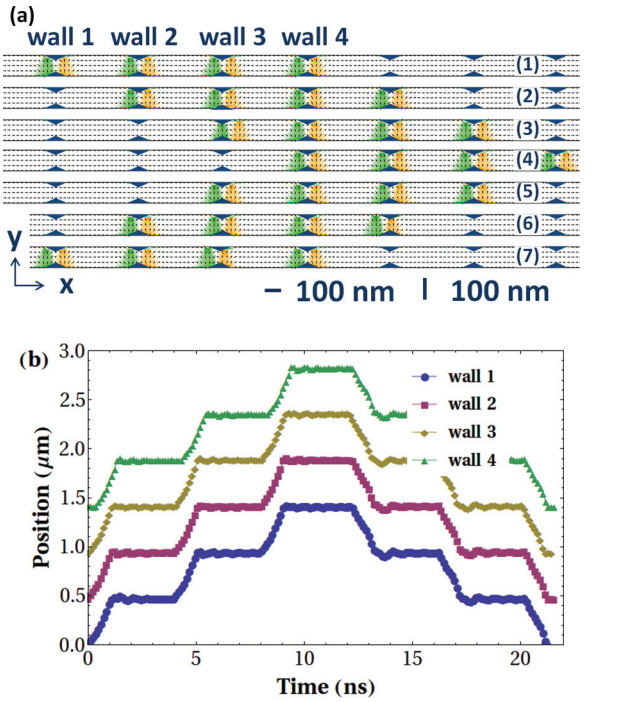

FIG. 5. (Color online) (a) Snapshots of coherent multiple 360° DW movement, with notch separation 470 nm, depth 12.5 nm, width 117 nm, $u = 500.0$ m/s, a pulse duration of 0.50 ns, and relaxation of 3.5 ns. In stages (3) and (5) it is possible to see that the walls are not exactly at the notch position. This is due to the relaxation stage bordering at its lower limit, whereas if there had been shorter relaxation time, the DWs would not have had enough time to stabilize at the notch, hence breaking the coherent motion. The magnetization pointing $-y$ is shown in green and the magnetization pointing $+y$ is shown in orange. (b) Position of multiple 360° DWs in time. The jumps in the position demarcate the DW movement when the spin current pulse is applied, until the next stable position at the notches is achieved.

observed a similar behavior when the stripe width was changed to 50 nm or 200 nm. This feature could be exploited to achieve an even greater DW density if this system is scaled to other dimensions.

On the other hand under the same conditions that are shown in Fig. 5, TDWs were not able to move in a synchronized way, as shown in Fig. 6, being annihilated instead. Finally, it was found that the minimum time for two 360° DWs to move and stabilize at the notches was 2.5 ns at a distance of 235 nm; on the other hand a distance of 1 μm and 8 ns were in the case of two TDWs.

E. Dynamical regime

In the dynamical regime we can estimate a maximum pulse duration for a given initial distance of two DWs, either TDWs or 360° DWs. Such an estimate is made based on the time that it takes for the DWs to recombine while the spin current is being applied, as shown in Fig. 7. It is worth noting that this analysis is valid if at the end of the pulse the DWs are located in the vicinity of a notch, which occurs for most cases for pulses between 0.75 and 1 ns. Once the DWs are pinned by the notch the description of the static regime becomes valid.

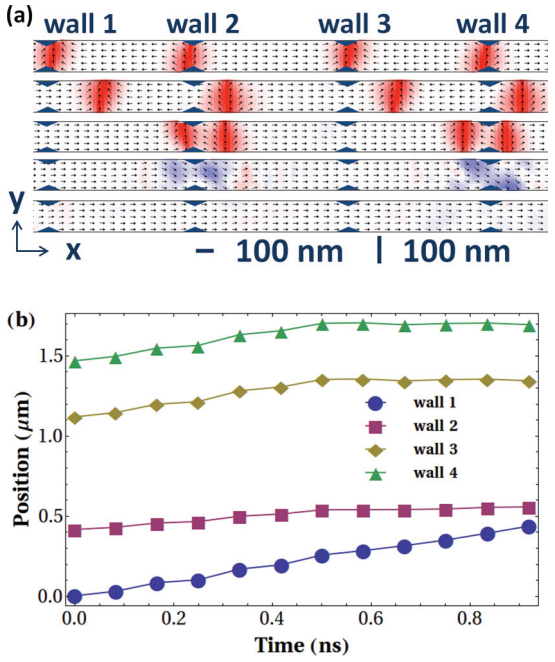

FIG. 6. (Color online) Notch width 117 nm, depth 12.5 nm, $u = 500.0$ m/s, spin current pulse duration 0.50 ns, and relaxation 3.5 ns. (a) Snapshots of multiple TDWs' movement from one notch to another. The two TDWs, unlike their 360° DW counterpart, rapidly annihilate after the spin current pulse is applied, taking about 0.9 ns to disappear under these conditions. The magnetization pointing $+y$ is shown in red and the magnetization pointing $-y$ is shown in blue. (b) DW position of the four walls depicted in (a), as they come closer and annihilate.

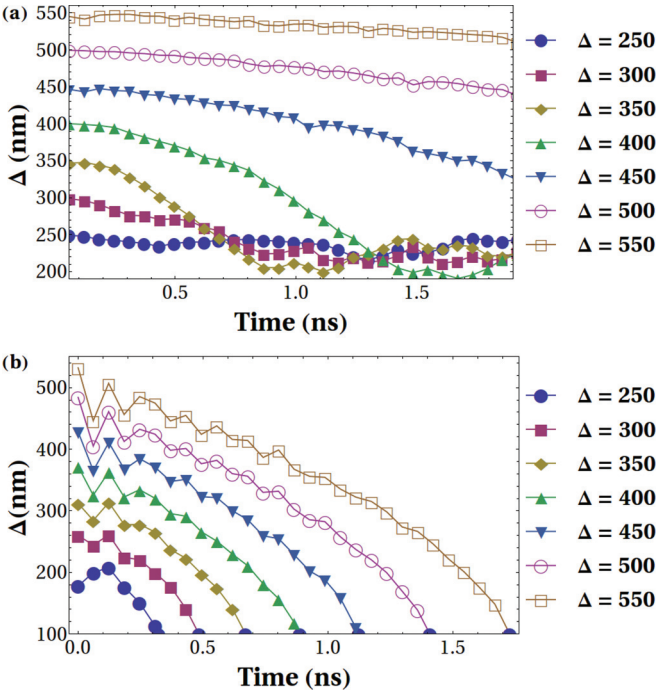

FIG. 7. (Color online) Recombination time for (a) 360° DWs and (b) TDWs and for different initial distance Δ, and a spin current of $u = 400$ m/s.

Although we do not take into account the notches during the recombination of the DWs, we can estimate it from our analysis as we are only interested in the dynamical regime where the DWs are moving outside the effect of the notches. In the case that the duration of the spin current pulse is longer than our estimate, the DWs would interact, recombining before they are pinned at the notches. Such behavior is undesirable in a system of these characteristics. We limited the analysis to a maximum time of 2 ns, which is almost twice the maximum time required for one 360° DW to reach the next notch.

In Fig. 7(a) we can see that for two 360° DWs initially located at about their static equilibrium distance, ∼250 nm, when the spin current pulse is applied they rebound with each other as they achieve their equilibrium distance. When the initial distance is increased to 300 nm, the recombination time is ∼0.6 ns; hence for such initial DW separation the time that it takes for them to move from one notch to another has to be shorter than this threshold in order to not allow the walls to recombine. For initial distances higher than 400 nm, the spin pulse could be applied up to 1.2 ns without the walls recombining during the process. Finally, we found that the recombination time was not heavily dependent on the velocity of the spin current used, varying at most 0.1 ns in the range of 100 to 700 m/s.

In Fig. 7(b) we can see how the annihilation of TDWs also depends on the initial distance. For the time duration of the spin current pulses, most of the separations ended in annihilation, although according to 7(b) when they are further away than 500 nm the DWs should be conserved. However, this does take not into account the simulations we performed considering a sequence of spin current pulses and the more important fact that the interaction of the walls does affect the pinning location of a TDW. For this reason, we can state that for these length scales TDWs are not suitable.

IV. CONCLUSIONS

In this paper we reported the static and dynamic behavior of TDWs and 360° DWs in a patterned nanostripe. Using the model developed by Allwood *et al.*,[12,22] we described the interaction between two TDWs and then between two 360° DWs, which was found to be dominated by the effect of their stray field. In the case of two TDWs the validity of the model spans most of the distances explored. On the other hand for 360° DWs at distances lower than two domain wall lengths the interaction changes abruptly, having its origins most probably in the deformation induced by the interaction between walls. Based on this phenomen we were able to estimate the shortest distance at which we could locate the notches and still have reliable control over the DW movement. On the other hand, based on the data obtained during the movement of DWs we estimated the cycling times for the system proposed.

Moreover, in terms of the parameters involved in the coherent domain wall motion, relevant factors were the depth and width of the notches, which controlled the spin current depinning value. A change in almost one and a half times the width resulted in only a 5% increase in the value of the depinning current, although a change of twice the depth reported about a 50% change. Using these values we applied

the same principles to an array of 360° DWs, achieving coherent DW motion. The description of the interaction of TDWs and 360° DWs allowed us to conclude that given the reduction of stray fields from the 360° DWs, their density can be a factor of four larger than in devices based on single transverse domain walls. This increase in density translates to a 50% reduction in write times which potentially gives our system important industrial applications. In terms of the outlook of this research, one of the main challenges ahead is to develop such a mechanism that allows us to locally nucleate 360° DWs which would allow us to have better control over the features involved in the nucleation of the 360° DWs.

ACKNOWLEDGMENTS

This work was funded by the Government of Chile through Conicyt and its program, Becas Chile. Furthermore, the calculations were carried out using the Camgrid high-throughput facility of the University of Cambridge. This work was performed using the Darwin Supercomputer of the University of Cambridge High Performance Computing Service, provided by Dell, Inc., using Strategic Research Infrastructure Funding from the Higher Education Funding Council for England and funding from the Science and Technology Facilities Council. Finally, the authors would like to thank T. Yu and Stuart Holmes for their useful advice.

*alg55@cam.ac.uk

[1] S. Konishi, Magnetics, IEEE Trans. Magn. **19**, 1838 (1983).
[2] R. Katti, J. Wu, and H. Stadler, in 2nd NASA SERC Symposium on VLSI Design, No. N94-71129, 1990.
[3] Stuart S. P. Parkin, H. Masamitsu, and T. Luc, Science **320**, 190 (2008).
[4] Stuart S. P. Parkin, X. Jiang, C. Kaiser *et al.*, Proc. IEEE **91**, 661 (2003).
[5] X. Jiang, L. Thomas, R. Moriya *et al.*, Nat. Commun. **1**, 25 (2010).
[6] G. Hrkac, J. Dean, and D. A. Allwood, Philos. Trans. R. Soc., A **369**, 3214 (2011).
[7] R. Cowburn, in *International Conference on Electromagnetics in Advanced Applications, 2007* (ICEAA, San Francisco, USA, 2007), p. 602.
[8] M. Hayashi, L. Thomas, C. Rettner, R. Moriya, and Stuart S. P. Parkin, Nat. Phys. **3**, 21 (2007).
[9] L. O'Brien, D. Petit, E. R. Lewis, R. P. Cowburn, D. E. Read, J. Sampaio, H. T. Zeng, and A.-V. Jausovec, Phys. Rev. Lett. **106**, 087204 (2011).
[10] A. Kunz and Jonathan D. Priem, IEEE Trans. Magn. **46**, 1159 (2010).
[11] A. Kunz and E. W. Rentsch, IEEE Trans. Magn. **46**, 1156 (2010).
[12] T. J. Hayward, M. T. Bryan, P. W. Fry, P. M. Fundi, M. R. J. Gibbs, D. A. Allwood, M.-Y. Im, and P. Fischer, Phys. Rev. B **81**, 020410 (2010).
[13] Mark D. Mascaro, Chunghee Nam, and C. A. Ross, Appl. Phys. Lett. **96**, 162501 (2010).
[14] A. L. Gonzalez Oyarce, T. Trypiniotis, P. E. Roy, and C. H. W. Barnes, Phys. Rev. B **87**, 174408 (2013).
[15] C. B. Muratov and V. V. Osipov, IEEE Trans. Magn. **45**, 3207 (2009).
[16] A. Goldman, A. S. Licht, Y. Sung, Y. Li *et al.*, J. Appl. Phys. **111**, 07D113 (2012).
[17] L. J. Heyderman, H. Niedoba, H. O. Gupta, and I. B. Puchalska, J. Magn. Magn. Mater. **96**, 125 (1991).
[18] C. B. Muratov and V. V. Osipov, J. Appl. Phys. **104**, 053908 (2008).
[19] L. O'Brien, D. Petit, H. T. Zeng, E. R. Lewis, J. Sampaio, A. V. Jausovec, D. E. Read, and R. P. Cowburn, Phys. Rev. Lett. **103**, 077206 (2009).
[20] A. Kunz, Appl. Phys. Lett. **94**, 132502 (2009).
[21] Oleg Tchernyshyov and Gia-Wei Chern, Phys. Rev. Lett. **95**, 197204 (2005).
[22] T. J. Hayward, M. T. Bryan, D. A. Allwood *et al.*, Appl. Phys. Lett. **96**, 052502 (2010).
[23] A. L. Gonzalez Oyarce, J. Llandro, Y. Nakatani, and C. H. W. Barnes (unpublished).
[24] Y. Jang, S. R. Bowden, Mark Mascaro, J. Unguris, and C. A. Ross, Appl. Phys. Lett. **100**, 062407 (2012).
[25] M. Diegel, R. Mattheis, and E. Halder, IEEE Trans. Magn. **40**, 2655 (2004).
[26] M. J. Donahue and D. G. Porter, Interagency Report NISTIR 6376, OOMMF User's Guide, Ver. 1.0, Technical Report, National Institute of Standards and Technology, Gaithersburg, MD, 1999.
[27] W. F. Brown, *Micromagnetics* (Interscience Publishers, New York, USA, 1963).
[28] H. Kronmuller and M. Fahnle, *Micromagnetism and the Microstructure of Ferromagnetic Solids* (Cambridge University Press, Cambridge, UK, 2009).
[29] *Handbook of Magnetism and Advanced Magnetic Materials*, edited by H. Kronmüller and S. Parkin, Vol. 2, *Micromagnetism* (Wiley, New York, USA, 2007).
[30] J. C. Slonczewski, W. Palmer, M. H. Francombe, and A. J. Heeger, *Magnetic Materials Digest*, edited by A. H. Morrish, R. J. Prosen, and S. M. Rubens (AIP, New York, 1961).
[31] G. Nahrwold, J. M. Scholtyssek, S. Motl-Ziegler *et al.*, J. Appl. Phys. **108**, 013907 (2010).
[32] Mark D. Mascaro and C. A. Ross, Phys. Rev. B **82**, 214411 (2010).
[33] J. Miltat A. Thiaville, Y. Nakatani, and Y. Suzuki, Europhys. Lett. **69**, 990 (2005).